

A RECONFIGURABLE CEDAR-SHAPED MICROSTRIP ANTENNA FOR WIRELESS APPLICATIONS

M. A. Madi, M. Al-Husseini^{*}, A. H. Ramadan, K. Y. Kabalan, and A. El-Hajj

ECE Department, American University of Beirut, P. O. Box 11-0236, Bliss Street, Beirut 1107 2020, Lebanon

Abstract—This paper presents a frequency reconfigurable cedar-shaped fractal antenna. The special shape of the patch makes it simpler to integrate RF switches to connect consecutive branches. The proper activation/deactivation of the switches alters the current flow and changes the resonance frequency. Simulated and measured results show the characteristics of the presented design.

1. INTRODUCTION

Research in electromagnetism and antenna design has focused on improving the antenna characteristics to fit modern telecommunications demands for miniaturized antennas that operate over multiple bands [1]. The tendency of grouping many services in an increasingly narrow space has made fractal antenna design a research hotspot. On the other hand, maintaining acceptable radiation pattern and gain characteristics, and improving noise mitigation, has led to focus on reconfigurability techniques.

Fractal theory, proposed by B. Mandelbrot, states that the space can have a fractional dimension that is in contrast with Euclidean space [2]. Fractal geometry is based on self repetition leading to infinitely fine structures thus simulating natural elements [2]. The space-filling property results in miniaturizing classic antenna elements. Another characteristic of fractal shapes is the self-similarity property employed to maintain antenna characteristics [3, 4]. Fractals can best be generated by iterating a certain shape with an increasingly reduced scale for consecutive iterations. As a result, the electrical length of the antenna increases causing the resonant frequency to be lowered achieving physical reduction of the antenna.

Received 12 October 2011, Accepted 17 November 2011, Scheduled 24 November 2011

* Corresponding author: Mohammed Al-Husseini (husseini@ieee.org).

Various fractal shapes have been implemented to design compact-sized antennas. In a nested triangle [2], the height and angle of the largest triangle and the number of nested triangles are varied to obtain the desired pass-band characteristics of the antenna. Koch-based fractal is exploited with two iterations in [5] to achieve a good axial ratio, where as in [6], a second-iterated Sierpinski carpet is used to obtain ultra wide band operation. In [4], natural structures with one or more iterations have been used to show the efficiency of using fractal shapes in designing antennas that respond to telecommunication system developments and the need for portable devices.

Grouping many services in one antenna, using the reconfigurability approach, results in better isolation of antennas and hence, increases the efficiency of modern platforms. In particular, due to their improved out of band rejection, frequency reconfigurable antennas surpass multiband antennas as they do not necessitate highly efficient noise filters and thus the cost of the overall antenna is reduced [1]. Employing frequency reconfigurable antennas also preserves the radiation properties at the various reconfigured frequencies. Frequency reconfigurability is usually achieved by incorporating switches across slots such as MEMS switches and p-i-n diodes. In [7], the authors present a PCB with electronic switches placed across slots in the feed line for Cognitive Radio applications. Optical switching was also used in [8] to obtain frequency reconfigurability where laser diodes were embedded in the substrate.

In general, the switches use de-biased signals to change the current path and to shorten the electrical length of the antenna [1]. Switches could be used to vary the depth of slots [9] which varies the electrical length of the antenna and consequently its resonant frequency. They may also be used to control the current flow path within two different configurations printed on the same patch, such as an inner and an outer square patch [10]. Compared to p-i-n diodes, RF MEMS switches consume less power and perform better but are still costly, so when used they are subject to optimization in positioning and quantity. Compared to p-i-n diodes, RF MEMS switches consume less power and perform better but are still costly, so when used they are subject to optimization in positioning and quantity [1]. Some configurations are adapted to host electronic switches due to their richness. A Vivaldi antenna is used by the authors in [11] to incorporate four pairs of p-i-n diodes. A dual frequency reconfigurable TLLPD (tunable loop-loaded printed dipole) is reported in [12]. The authors in [13] present an antenna with band notch reconfigurability based on complementary split-ring resonators (CSRRs) and split-ring resonators (SRRs).

Designing a fractal antenna in combination with reconfigurability

approach that incorporates electronic switches has produced more efficient antennas with size reduction. The authors of [14] apply a Koch curve to a U-slotted square patch to obtain wide band frequency reconfigurability. In [15], the authors use Sierpinski triangles to build a fractal Gasket-shaped frequency reconfigurable antenna.

This paper adopts a cedar-shaped microstrip antenna which is characterized by its fractal geometry that allows for a wide range of possibilities for placing RF switches. The antenna design is based on having pairs of symmetrical slots to form branches. Switches mounted over these slots could be activated to obtain frequency reconfigurability. The space filling property and self similarity of the fractal shape have served to decrease the antenna's operation frequencies and to keep the consistency of its radiation patterns, respectively.

2. ANTENNA DESIGN

An equilateral patch antenna is first designed to resonate at 2.4 GHz. The relation between the dimension of an equilateral triangle patch and the resonant frequency is given in Equation (1) [16]. A side length of 38.86 mm (height = 33.65 mm) is obtained.

$$f_{mnl} = \frac{2c}{3a(\epsilon_r)^{1/2}} (m^2 + mn + n^2)^{1/2} \tag{1}$$

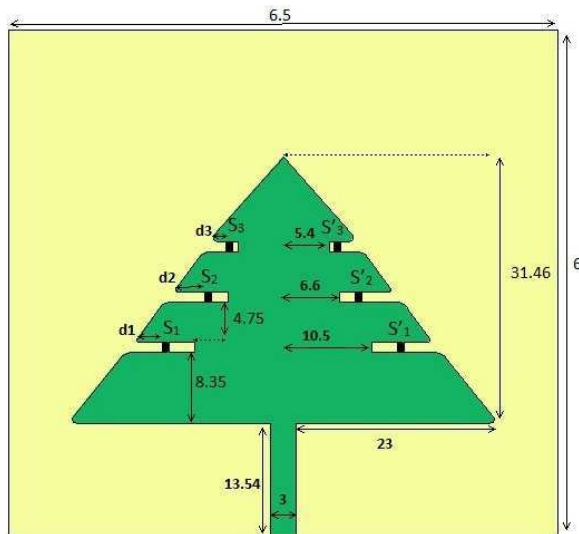


Figure 1. Antenna geometry (dimensions in mm).

In (1), c is the velocity of electromagnetic waves in free space, ϵ_r is the dielectric constant of the substrate, m , n , and l are the integers corresponding to the mode, and a is the side length of the equilateral triangle.

Trims are to be symmetrically incorporated into the triangular patch to form the branches of the cedar. To give more area to these trims, and to keep the matching at around 2.4 GHz, the base of the patch (side connected to the feed line) has to be elongated, and the height has to be shortened. For three trims on each side, the optimizations lead to a base length and a height of 49 mm and 31.5 mm, respectively.

Further optimizations are done to ensure positive gain and also for aesthetic reasons. The final design, which now has the shape of a cedar tree, is printed on an FR4-epoxy substrate with a dielectric constant $\epsilon_r = 4.4$, and has a full ground plane, and a 50- Ω matched microstrip feed line. Three pairs of switches are mounted across the trims to control the current flow on the patch. The detailed antenna is described in Figure 1.

A parametric study for the positions of the switches is done, and a prototype based on selected locations of the switches is fabricated, as demonstrated in the next section.

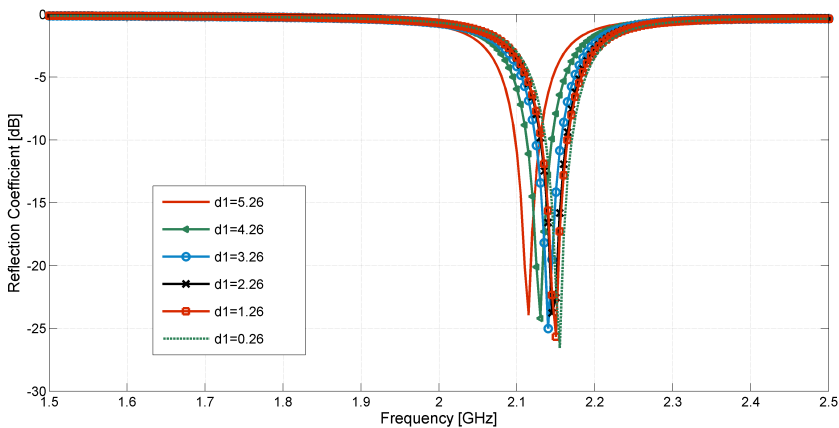


Figure 2. S_{11} results for variable positions of (S_1, S'_1) with (S_2, S'_2) and (S_3, S'_3) in the OFF state.

3. RESULTS AND DISCUSSION

The design and parameter optimization are done using Ansoft HFSS [17], which is based on the Finite-Element Method (FEM). The measurements are done using Agilent’s E5071B network analyzer.

Since the positions of the switches affect the current flow path, varying these positions certainly tunes the obtained resonance frequency. The positions of the switches are denoted d_1 , d_2 , and d_3 , as shown in Figure 1, and a parametric study is done to show the effect of a switch position of the antenna’s resonance.

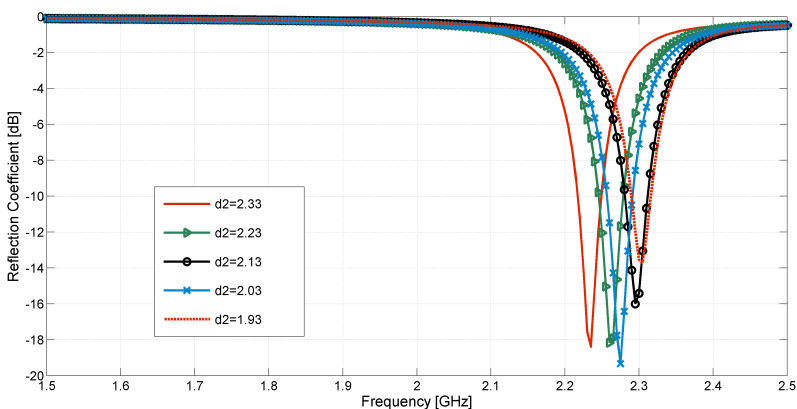


Figure 3. S_{11} results for variable positions of (S_2, S'_2) with (S_1, S'_1) in the ON state at $d_1 = 2.26$ mm and (S_3, S'_3) in the OFF state.

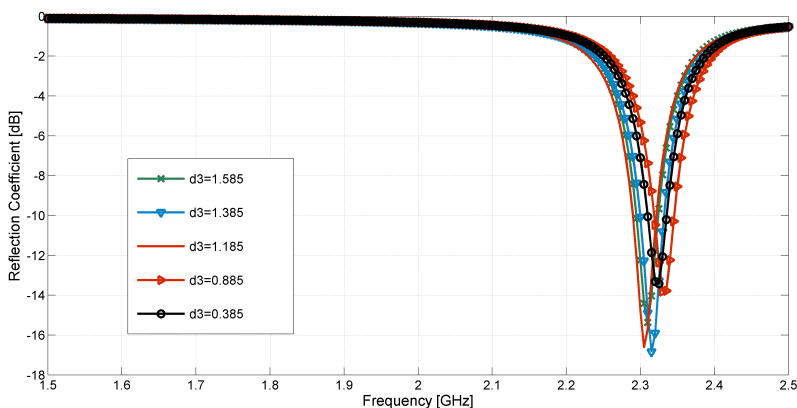


Figure 4. S_{11} results for variable positions of (S_3, S'_3) with (S_1, S'_1) and (S_2, S'_2) in the ON state at $d_1 = 2.26$ mm and $d_2 = 2.13$ mm.

First, switches (S_1, S'_1) are turned ON and switches (S_2, S'_2) and (S_3, S'_3) are turned OFF. Then switches (S_1, S'_1) are placed at several positions, and the corresponding resonance frequency is obtained. The reflection coefficient plots for 6 different d_1 values are given in Figure 2. They show that the resonance frequency increases with decreasing d_1 value.

Fixing the positions of (S_1, S'_1) at $d_1 = 2.26$ mm, (S_2, S'_2) are moved over 5 different positions achieving frequency tunability in

Table 1. Switch states for Cases 0, 1, 2, and 3.

Case	(S_1, S'_1)	(S_2, S'_2)	(S_3, S'_3)	Resonance Frequency (GHz)	Gain (dB)
0	OFF	OFF	OFF	2.075	0.2798
1	ON	OFF	OFF	2.145	1.0373
2	ON	ON	OFF	2.295	2.1824
3	ON	ON	ON	2.325	2.5098

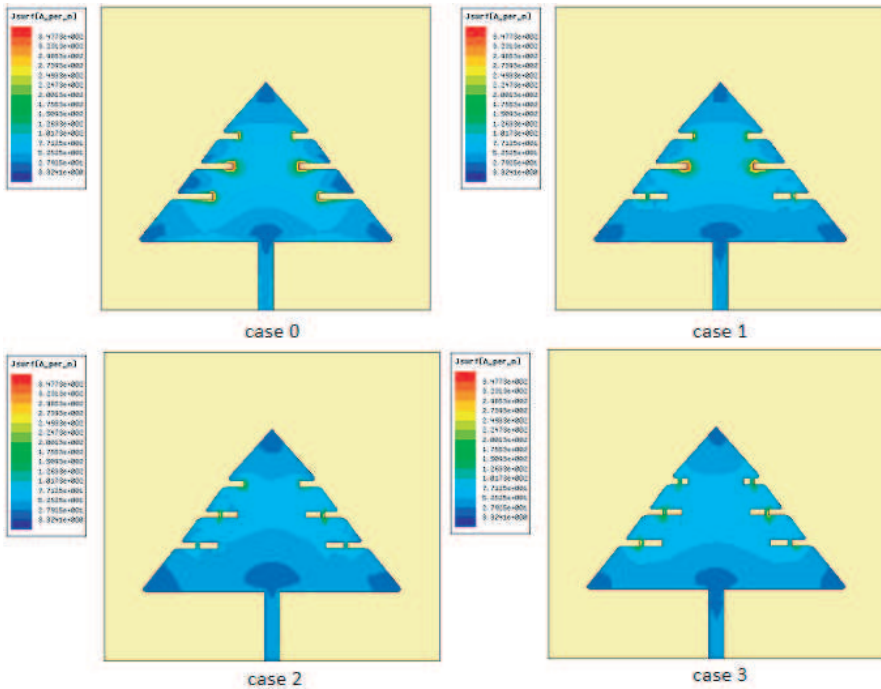


Figure 5. Current distribution for switching Cases 0, 1, 2, and 3 presented in Table 1.

2.235–2.305 GHz frequency band as shown in Figure 3. The resonance frequency increases with decreasing d_2 value.

Similarly, the positions of the first two pairs of switches are fixed at $d_1 = 2.26$ mm and $d_2 = 2.13$ mm while (S_3, S'_3) are moved in 5 switching cases to tune the antenna in 2.305–2.335 GHz band as shown in Figure 4.

The locations of the switches are chosen such as $d_1 = 2.26$ mm, $d_2 = 2.13$ mm and $d_3 = 0.385$ mm (refer to Figure 1). The successive activation of each pair of switches, from bottom to top, results in altering the flow of current and as a result in shifting the resonance frequency. Four switching cases are chosen, as listed in Table 1. The current distribution on the patch for these cases is shown in Figure 5. When a switch is OFF, the current flows around the corresponding trim, thus its path is longer, and the resonance frequency is lower.

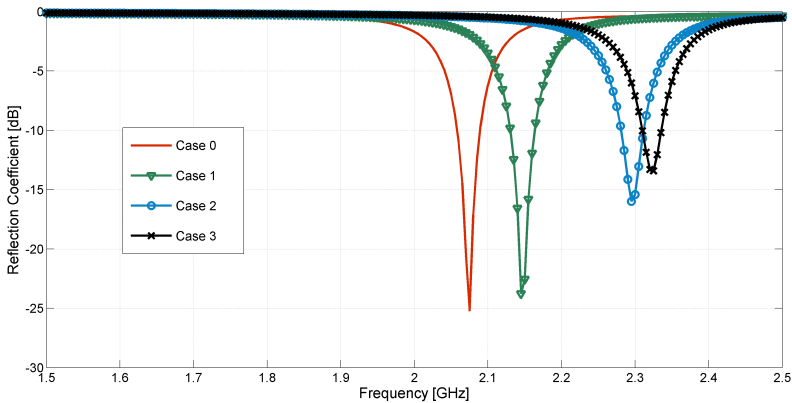


Figure 6. Simulated S_{11} of the antenna for switching Cases 0, 1, 2 and 3.



Figure 7. Cedar prototype for Case 3 described in Table 1.

Simulated S_{11} plots in Figure 6 show frequency reconfigurability at 2.075 GHz, 2.145 GHz, 2.295 GHz, and 2.325 GHz for the different switching cases. A prototype of the antenna is fabricated. A photo of the prototype is shown in Figure 7.

The measured S_{11} plots are shown in Figure 8. They are in very good agreement with the simulated ones.

In the results of Figures 6 and 8, switches in their ON state were replaced by $1.2\text{ mm} \times 0.8\text{ mm}$ copper strips. In the OFF state, the copper strips were removed. The technique of replacing electronic switches by copper strips in simulations is reported as

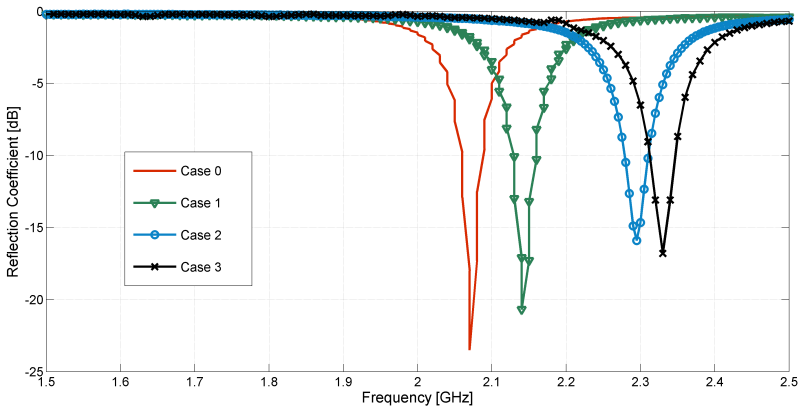


Figure 8. Measured S_{11} for switching Cases 0, 1, 2 and 3.

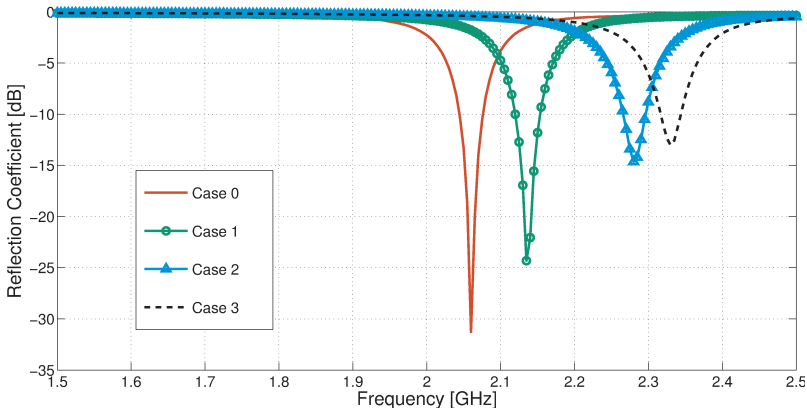


Figure 9. Simulated S_{11} for switching Cases 0, 1, 2 and 3 using reed switch model.

valid in [14, 18, 19]. Using real switches, such as p-i-n diodes or RF MEMS, requires the design of their biasing networks. These biasing networks will leave their effect on the antenna's characteristics, especially the radiation patterns. However, some other types of switches do not need such biasing lines. They are actuated from below the ground plane, without affecting the radiation patterns. These include photoconductive switches [8], and reed switches [20, 21].

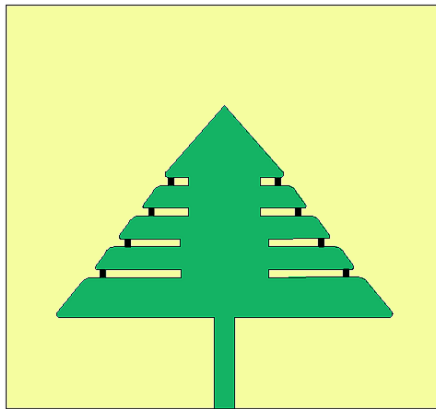


Figure 10. Design with more trims that widens the frequency reconfigurability band.

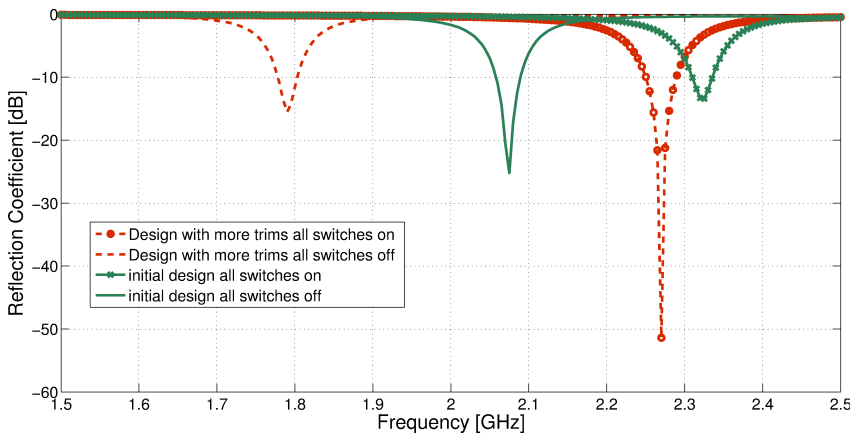


Figure 11. Simulated S_{11} of the new antenna design shown in Figure 10 for two switching cases (all switches OFF and all switches ON) in comparison with the initial design.

In [20], a Reed switch was modeled as a $0.2\text{-}\Omega$ resistance when in the ON state, and as a 0.1 pF capacitance in the OFF state. Using this model in the simulations, the S_{11} plots in Figure 9 are obtained. These results are almost identical to the ones in Figure 6, hence the validity of using the copper strip model.

The number of trims in the patch and their depth directly affect the difference in the electrical length between Case 0 and Case 3, and hence the frequency reconfigurability range. A wider frequency reconfigurability range is obtained by increasing the number of trims and/or making them deeper. An example modified design is shown

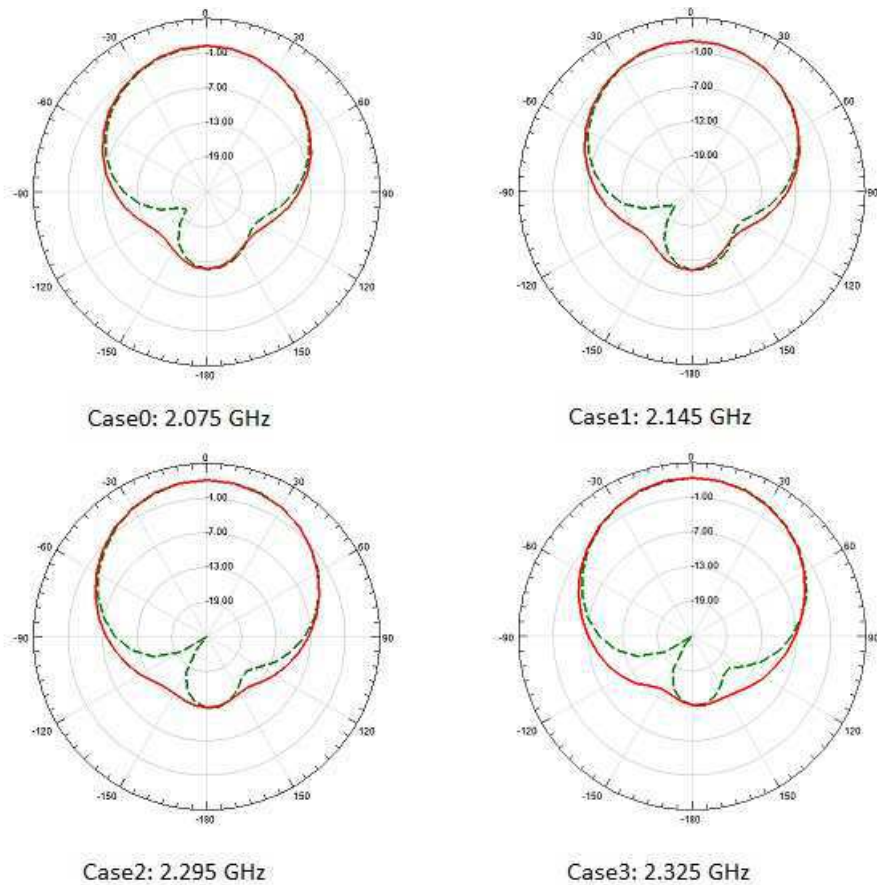


Figure 12. Radiation pattern of the antenna in the H -plane (solid line) and E -plane (dashed line) for the adopted switching cases.

in Figure 10. A comparison of the reflection coefficient plots for Cases 0 and 3 of the original design and the modified design are given in Figure 11. It is shown that a 92% increase in the frequency reconfigurability range is achieved. More deeper trims will further increase this range.

For the design in Figure 1, the computed gain patterns in the E - and H -planes, for each of the switching cases, are shown in Figure 12. The four switching cases result in broadside patterns that remain consistent over the four obtained operation bands. The obtained peak gain values are given in Table 1.

4. CONCLUSION

A cedar-shaped fractal antenna with frequency reconfiguration ability was presented. The space-filling property of the antenna served to lower its resonant frequency, and its self-similarity property to keep consistent some of its characteristics. Frequency reconfigurability was obtained by mounting and activating switches between the different branches of the cedar. The switches allow modifying the current path, and as a result the obtained resonance frequency. The frequency reconfigurability range for the fabricated prototype is 2–2.4 GHz but can be adjusted by modifying the number and depth of the incorporated trims. Simulated and measured results were in agreement.

REFERENCES

1. Yang, S., Z. Chunna, P. Helen, A. Fathy, and V. Nair, "Frequency-reconfigurable antennas for multiradio wireless platforms," *IEEE Microwave Magazine*, Vol. 10, No. 1, 66–83, Feb. 2009.
2. Yu, Y. H. and C. P. Ji, "Research of fractal technology in the design of multi-frequency antenna," *Microwave Conference Proceedings (CJMW)*, 1–4, Apr. 2011.
3. Ramadan, A., M. Al-Husseini, K. Y. Kabalan, and A. El-Hajj, "Fractal-shaped reconfigurable antennas," *Microstrip Antennas*, N. Nasimuddin (ed.), ISBN 978-953-307-247-0, InTech, Apr. 2011.
4. Balanis, C. A., *Antenna Theory, Analysis and Design*, John Wiley and Sons, 2005.
5. Rao, P. N. and N. V. S. N. Sarma, "A single feed circularly polarized fractal shaped microstrip antenna with fractal slot," *PIERS Proceedings*, 195–197, Hangzhou, China, Mar. 24–28, 2008.

6. Ramadan, A., M. Al-Husseini, K. Y. Kabalan, A. El-Hajj, and J. Costantine, "A compact Sierpinski-carpet-based patch antenna for UWB applications," *Proceedings of IEEE Antennas and Propagation Society International Symposium (APS-URSI 2009)*, 1–4, Jun. 2009.
7. Al-Husseini, M., A. Ramadan, M. E. Zamudio, C. G. Christodoulou, A. El-Hajj, and K. Y. Kabalan, "A UWB antenna combined with a reconfigurable bandpass filter for cognitive radio applications," *The 2011 International Conference on Electromagnetics in Advanced Applications (ICEAA2011)*, Torino, Italy, Sep. 12–16, 2011.
8. Tawk, Y., M. Al-Husseini, S. Hemmady, A. R. Albrecht, G. Balakrishnan, and C. G. Christodoulou, "Implementation of a cognitive radio front-end using optically reconfigurable antennas," *The 2010 International Conference on Electromagnetics in Advanced Applications (ICEAA2010)*, Sydney, Australia, Sep. 20–24, 2010.
9. Cai, X., A. Wang, and W. Chen, "A circular disc-shaped antenna with frequency and pattern reconfigurable characteristics," *2011 China-Japan Joint Microwave Conference Proceedings (CJMW)*, 1–4, Apr. 2011.
10. De Luis, J. R. and F. de Flaviis, "A reconfigurable dual frequency switched beam antenna array and phase shifter using PIN diodes," *IEEE Antennas and Propagation Society International Symposium, 2009, APSURSI'09*, 1–4, Jun. 2009.
11. Hamid, M. R., P. S. Hall, P. Gardner, and F. Ghanem, "Frequency reconfigurable Vivaldi antenna," *2010 Proceedings of the Fourth European Conference on Antennas and Propagation (EuCAP)*, 1–4, Apr. 2010.
12. Sondas, A., M. H. B. Ucar, and Y. E. Erdemli, "Tunable loop-loaded printed dipole antenna design," *Antennas and Propagation Society International Symposium (APSURSI)*, 1–4, Jul. 2010.
13. Al-Husseini, M., J. Costantine, C. G. Christodoulou, S. E. Barbin, A. El-Hajj, and K. Y. Kabalan, "A reconfigurable frequency-notched UWB antenna with split-ring resonators," *Microwave Conference Proceedings (APMC)*, 618–621, Dec. 2010.
14. Ramadan, A., K. Y. Kabalan, A. El-Hajj, S. Khoury, and M. Al-Husseini, "A reconfigurable U-Koch microstrip antenna for wireless applications," *Progress In Electromagnetics Research*, Vol. 93, 355–367, 2009.
15. Anagnostou, D. E., G. Zheng, M. T. Chryssomallis, J. C. Lyke, G. E. Ponchak, J. Papapolymerou, and C. G. Christodoulou,

- “Design, fabrication, and measurements of an RF-MEMS-based self-similar reconfigurable antenna,” *IEEE Transactions on Antennas and Propagation*, Vol. 54, No. 2, 422–432, Feb. 2006.
16. Guney, K., “Resonant frequency of a triangular microstrip antenna,” *Microwave and Optical Technology Letters*, Vol. 6, No. 9, Jul. 1993.
 17. Ansoft HFSS, Pittsburg, PA 15219, USA.
 18. Costantine, J., C. G. Christodoulou, and S. E. Barbin, “A new reconfigurable multi band patch antenna,” *SBMO/IEEE MTT-S International Microwave and Optoelectronics Conference, 2007, IMOC 2007*, 75–78, Oct. 2007.
 19. Zammit, J. A. and A. Muscat, “Tunable microstrip antenna using switchable patches,” *Antennas and Propagation Conference, 2008, LAPC 2008*, 233–236, Loughborough, Mar. 2008.
 20. Wu, C., T. Wang, A. Ren, and D. G. Michelson, “Implementation of reconfigurable patch antennas using reed switches,” *IEEE Antennas and Wireless Propagation Letters*, Vol. 10, 2011.
 21. <http://www.meder.com>.